Visibility analysis of man-made objects in SAR images

U. Soergel, U. Thoennessen and U. Stilla

***Abstract*— The increasing resolution of SAR data offers the possibility to utilize this data for a detailed scene interpretation in urban areas. Different SAR specific phenomena like foreshortening, layover, shadow and multipath-propagation burden the interpretation. A high resolution LIDAR DEM of an urban scene is incorporated to investigate the impact of the phenomena on the visibility of man-made objects by a SAR measurement from a given sensor trajectory and orientation. LIDAR data as ground truth is well suited for this task, because it contains elevation information of man-made and natural objects. Shadow and layover areas are simulated by incoherent sampling of the DEM. By a variation of viewing and aspect angles a large number of such simulations are carried out. From this set of segmentations the n best are determined with respect to the visibility of roads and buildings. Furthermore, the locations of total reflection or double-bounce scattering in the vicinity of buildings are determined.**

***Index Terms*—SAR, LIDAR, Simulation, Fusion.**

I. Introduction

SIDE-LOOKING scene illumination by SAR causes phenomena like foreshortening, layover, shadow, total reflection and multi-bounce scattering at elevated objects in the scene [4]. Due to the mostly vertical walls, these effects occur often at building locations. Especially in dense urban areas, large parts of the scene are often interfered with these phenomena. This may hinder the analysis of SAR images, particularly by automatic pattern recognition methods.

Algorithms for the detection and reconstruction of man-made objects from SAR and InSAR data have been proposed in the literature [1],[5],[7],[8]. In this context it is worthwhile to analyze to what extent man-made objects can be sensed with SAR in an urban environment. The focus here is on the visibility of roads and buildings. The analysis is based on vector maps provided by a GIS and elevation data.

The incorporation of elevation data in mission planning, geocoding and analysis of SAR imagery is investigated for many years. However, in the past often coarse digital terrain models (DTM) were available only (e.g. 30 m). This level of detail was sufficient for geocoding and interpretation of satellite SAR data with comparable ground resolution. Approaches for the simulation of layover and shadow areas from a given DTM were proposed for satellite data of rural scenes [3]. Layover and shadow regions are identified by sampling of the elevation data from a given sensor trajectory. Furthermore, the DTM was incorporated to simulate the influence of the terrain slope on a SAR measurement [2].

The increasing resolution of new SAR sensor systems gives rise for the need of more detailed elevation data. In urban areas CAD building descriptions can serve as ground truth for a simulation of layover and shadow areas [1]. Furthermore, from the orientation of the building planes the locations of multi-propagation and total reflection are predictable. CAD data sets are often restricted to man-made objects. But, even in dense urban areas natural objects like trees and bushes are present at many locations. Hence, their influence should be considered to avoid too optimistic estimates of the visibility of man-made objects. Information about natural objects are provided e.g. in first pulse LIDAR DEM. In order to combine the advantages of raster and vector height data, the building layer of a map is used to separate the buildings from the rest of a LIDAR DEM. At the building locations the planes of roofs and walls are reconstructed from the DEM [6].

Subject of this paper is the investigation of the visibility of man-made objects with SAR sensors in built-up areas. In Chapter II the illumination phenomena are discussed. Geometric constraints of their impact on the visibility of buildings and roads in SAR data are derived. Based on vector maps and a high resolution LIDAR DEM these effects are analyzed for an urban environment (Chapter III). An area

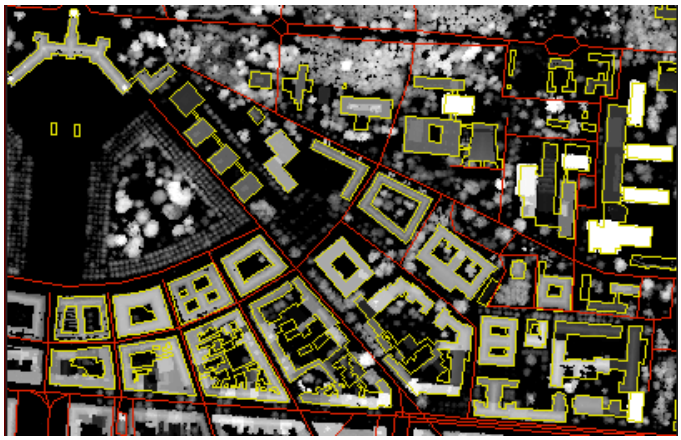

Fig. 1. LASER DEM superimposed by a vector map (roads and buildings)

U. Soergel, U. Thoennessen and U. Stilla are with the FGAN-FOM Research Institute for Optronics and Pattern Recognition, 76275 Ettlingen, Germany (e-mail: {soe,thoe,usti}@ fom.fgan.de).

covering the city center and university campus of Karlsruhe (Germany) was chosen as test site (Fig. 1). Assuming a special viewing angle and flight track, layover and shadow maps are calculated to determine the visibility of roads and building roofs. The results are compared with a high resolution SAR image of the scene.

The fusion of SAR measurements from different directions offers the opportunity to correct layover artifacts and to fill occluded areas. In order to demonstrate the benefit of such a multi-aspect scene analysis the simulations are carried out for a large number of different aspect and viewing angles. The optimal sets of several SAR acquisitions are determined. Total reflection and double-bounce are identified by analysis of 3D vector data. The results are discussed in Chapter IV.

II. APPEARANCE OF BUILDINGS IN SAR IMAGES

A. Phenomena caused by side-looking illumination

Fig. 2 illustrates typical effects in SAR images in the vicinity of buildings. The so-called layover phenomenon (Fig. 2a) occurs at locations with steep elevation gradient facing towards the sensor, like vertical building walls. Because object areas located at different positions have the same distance to the sensor, like roofs (I), walls (II) and the ground in front of buildings (III), the backscatter is integrated into the same range cell. Layover areas appear bright in the SAR image (Fig. 2c).

Perpendicular alignment of buildings to the sensor leads to strong signal responses by double-bounce at the dihedral corner reflector between the ground and the building wall (Fig. 2b). This results in a line of bright scattering in azimuth direction at the building footprint (Fig. 2c). At the opposite building side the ground is partly occluded from the building. This region appears dark in the SAR image, because no signal returns into the related range bins.

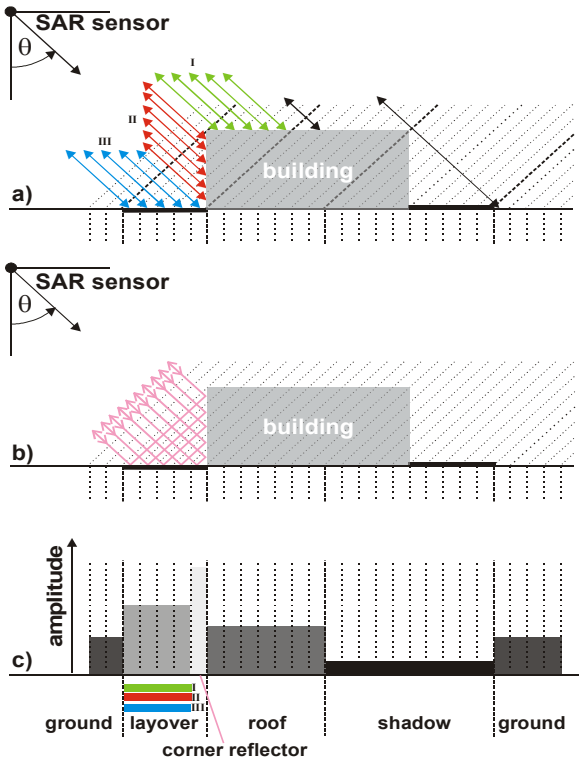

Fig. 2. SAR Phenomena at a flat roofed building: a) layover, b) corner reflector, c) range line of SAR image

Roof structures may lead to strong signal response as well. The gabled roof of the building sketched in Fig. 3 is oriented perpendicular towards the sensor. Since the entire power is mirrored back to the sensor, this total reflection leads to a line of dominant scattering in azimuth direction, similar to the corner reflector. This bright line caused from the roof appears closer to the sensor in the SAR image compared to the corner reflector. Besides the offset in range direction both effects can be discriminated by their polarimetric properties (single-bounce respectively double-bounce).

The mentioned effects can be studied in Fig. 4 comparing a section of an aerial image and a SAR image (the castle at the upper left side in Fig. 1). The SAR image is superimposed with the building footprints from a map. The scene was illuminated from top. The signal from the corner reflector at the castle's main building is located at the building footprint (1). The bright signal from the gabled roof is projected on the terrace in front of the castle (2). These two lines enclose the layover area. Layover can be observed as well at the castle wing (3) and at the tower (4), but no line of bright scattering appears, because the signal is reflected away from the sensor. Another double-bounce event happens at a little wall at the border of the terrace (5).

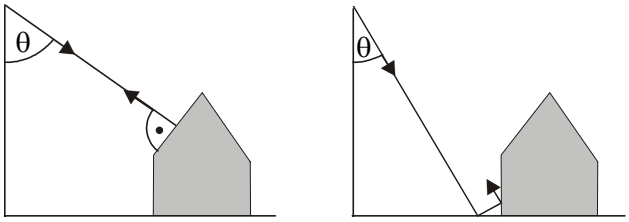

Fig. 3. Single (left) and double-bounce scattering at a gable roofed building

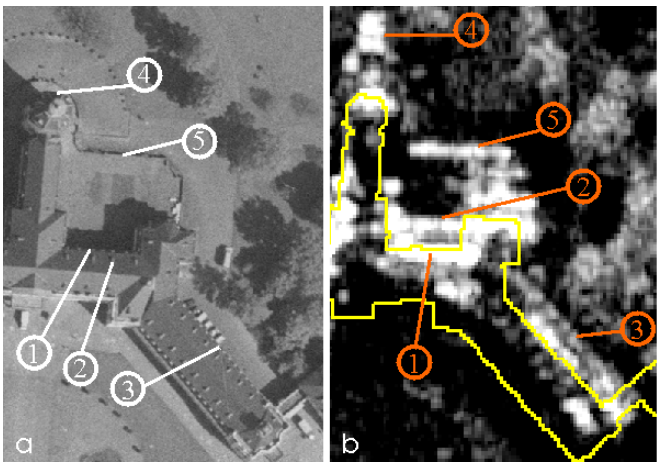

Fig. 4. Karlsruhe Castle: a) aerial image (1 main building wall, 2 main building roof, 3 wing, 4 tower, 5 terrace wall), b) SAR image overlaid with building footprints (yellow) and pointers to SAR phenomena (orange)

B. Geometric Constraints

In the following the phenomena of layover and shadow are discussed in more detail. The sizes of the layover areas l_g and shadow areas s_g on the ground in range direction depend on the viewing angle θ and the building height h. The layover area (see Fig. 5) is given by:

$$l_g = h \cdot \cot(\theta). \quad (1)$$

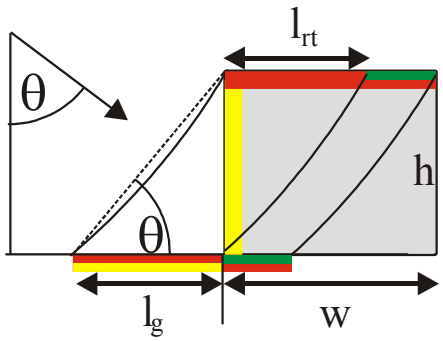

Fig. 5. Layover in front and on a flat roofed building

For the analysis of buildings the roof area l_{rt} is of interest which is influenced by layover. At the far side of a building with width w a part of the roof is not interfered with layover (shown in green in Figure 5) if the inequation is fulfilled:

$$h < w \cdot \tan(\theta). \quad (2)$$

In case of shadow geometric relations can be obtained too (Fig. 6). The slant range shadow length Δr is the hypotenuse of the rectangular triangle with the two sides h and s_g. Hence, the building elevation h can be directly obtained from:

$$h = \Delta r \cdot \cos(\theta). \quad (3)$$

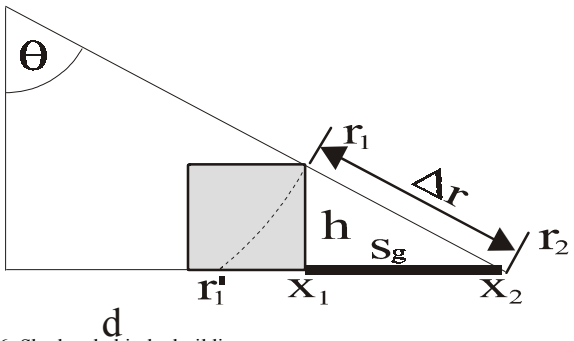

Fig. 6. Shadow behind a building

A simple projection of the slant range SAR data on a flat ground plane (ground range), ignoring the building elevation, leads to a wrong mapping of the roofs edge r_1 to point r_1'. Starting from point r_2 the true position x_1 of the building wall can be determined:

$$x_2 = r_2 \cdot \sin(\theta) \quad (4)$$

$$x_1 = x_2 - \Delta r \cdot \sin(\theta) \quad (5)$$

$$s_g = x_2 - x_1 = h \cdot \tan(\theta). \quad (6)$$

It is obvious, that at building locations a steep viewing angle leads to large layover areas on the ground and the roofs, but to small shadow areas and vice versa. Therefore, the viewing angle has to be chosen carefully.

The viewing angle increases in range direction over the swath. Assuming a viewing angle range between 40 and 60 degree, the shadow length of a certain building is more than doubled from near to far range. In Figure 7 such a situation is depicted (shadow length s_{gn}, s_{gf}). In the worst case a road between two building rows is orientated parallel to the sensor trajectory. The street is partly occluded from shadow and partly covered with layover. An object on the road can only be sensed properly if a condition for the road width w_s holds:

$$w_s > s_{gn} + l_g = h \cdot (\tan(\theta_{sn}) + \cot(\theta_l)). \quad (7)$$

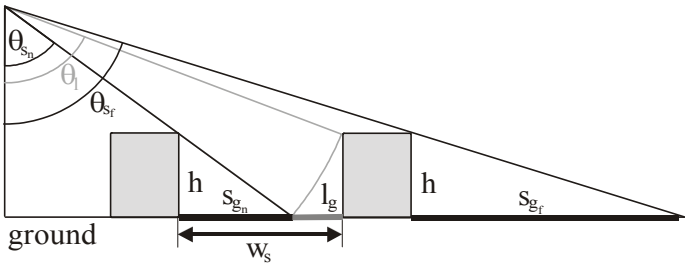

Fig. 7 Shadow and Layover from buildings displaced in range direction

In the sketch in Figure 7 the angle θ varies remarkable between the two buildings. In reality the angle changes only slightly over the width of a road. Hence, for the estimate of the size of the problem areas a constant θ is assumed. An angle of 55° in both cases and a building height of 20 m give a minimum w_s of 40 m.

III. SIMULATION OF SAR PHENOMENA

A. LIDAR data as ground truth

State of the art LIDAR systems achieve elevation accuracy in the decimeter scale on a meter grid or better on the ground. The elevation is derived from a time-of-flight measurement of infrared laser pulses emitted in nadir direction. The typical footprint diameter of the signal on the ground is approx. 30 cm (300 m altitude, beam divergence 1 mrad). At trees the signal is usually partly scattered from the canopy and from the ground beneath.

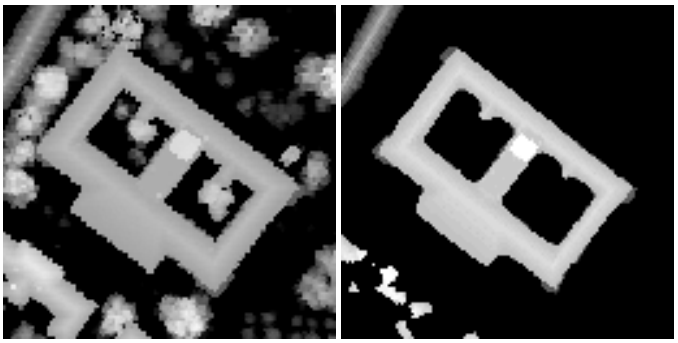

Fig. 8. LIDAR data: first pulse (left), last pulse (right)

The backscatter signal can be recorded in "first pulse" or "last pulse" mode (Fig. 8). Since the first pulse data represents the canopy better, this kind of data is suitable for the analysis of shorter radar wavelength signals which are mostly scattered from the canopy, e.g. X-band. In case of a longer radar wavelength, like L-band or P-band, last pulse LIDAR data is the better choice.

B. Simulation of Shadow and Layover

Meier et al. (1993) proposed an approach to simulate shadow and layover areas for satellite SAR data based on DTM as ground truth. This method was adopted for urban areas and high resolution DEM. The part of the scene that can be sensed reliably from a given sensor position is determined. The analysis is restricted to the geometric alignment of the scene towards the sensor, neglecting antenna side lopes and the aspect variation over the synthetic aperture. The elevation grid is sampled in range direction. For each bin the distance and viewing angle towards the sensor are calculated. These results are analyzed to determine shadow and layover areas.

The use of a coarse DTM restricts the approach to the terrain slope (macro scale level), which is often sufficient for satellite data. For an analysis of high resolution SAR data of urban scenes, elevated objects (meso scale level) have to be considered as well. Even in dense urban areas trees may cover large portions of the terrain. Neglecting the influence of natural objects might result in too optimistic estimates of the visibility of man-made objects. The SAR test data illustrated in Fig 9 was acquired in the X-band (HH polarization, ground resolution approx. 1m, $\theta = 55°$, sensor altitude 3000m). First pulse LIDAR data was chosen as ground truth to consider the canopy.

A simulation of shadow and layover areas with the given SAR parameters is illustrated in Fig. 10. Details are given in Table I. The large viewing angle suggests a larger portion of shadow compared to layover. This would be the case if all objects in the scene were detached not interfering the signal of each other. But, in the test scene the ground distance in range direction between the objects is often small. This results in many mixed pixels where shadow and layover are both present. Less than 20% of the road area can be sensed undisturbed. Especially for a building reconstruction from InSAR data, the influence of layover on the elevation measurement has to be considered. Due to the signal mixture, the elevation data tend to be too small at layover locations (neglecting the noise influence). Only 43% of the roof area is not interfered with layover or shadow.

TABLE I
RESULT OF SHADOW/LAYOVER SIMULATION IN PER CENT

	Complete scene	Roads	Building roofs
Shadow	28	38.5	16
Layover	25	18.5	33.5
Mixed	19	23.5	7.5
Reliable	28	19.5	43

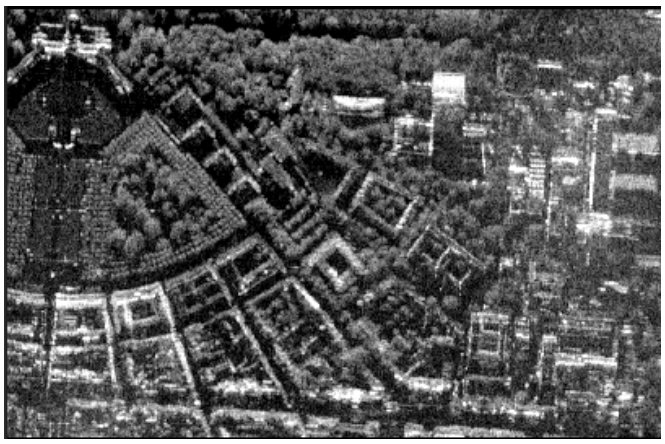

Fig. 9. SAR image (X-Band, HH-Pol., approx. 1m ground resolution)

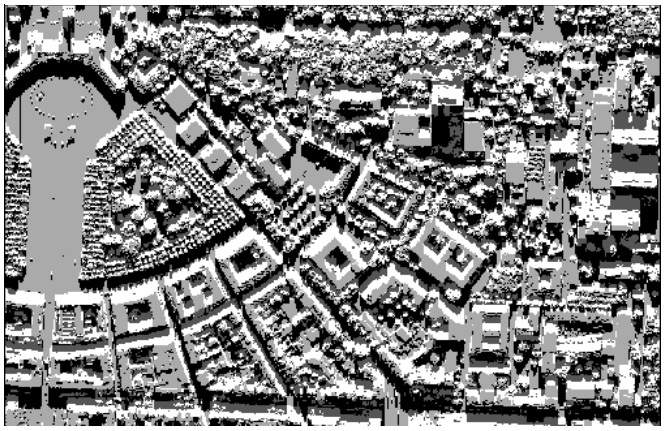

Fig. 10. Simulation with the given SAR parameters: Layover (white), shadow (black), layover and shadow (dark grey) and reliable data (bright)

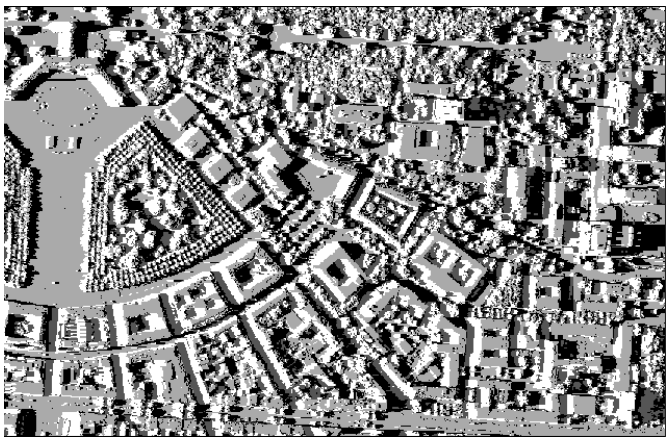

Fig. 11. Layover/shadow simulation for a SAR illumination from west

1) Potential of fusion of SAR data from different aspect and viewing angles

In order to estimate the improvement by incorporating additional SAR measurements acquired from different aspects a large number of simulations were carried out. The aspect angle was altered in steps of 5 degrees. For each of the 72 aspect directions the layover and shadow areas were detected

for 9 different viewing angles. The viewing angle θ was chosen between 30° and 70° with 5° increment. This results in 648 simulations. From this set the best single acquisition and the best set of two, three and four complementing SAR measurements were determined. The portion of useful signal from the entire road respectively building area was chosen as quality measure. The result for the best single measurement and for the fusion of 2, 3, and 4 SAR acquisitions is shown in Table II.

TABLE II
PORTION OF VISIBLE ROOF AND ROAD AREA FOR THE OPTIMAL SINGLE AND COMBINATION OF SEVERAL SAR ACQUISITIONS IN PER CENT

SAR measurements	1	2	3	4
Visible roof area	51.6	72.8	81.5	86.5
Visible road area	39	47	55.6	62

The optimal four aspects with respect of the visibility of buildings are oriented along the cardinal directions in the order east, north, west and south, with viewing angle 60 degree except for the north direction (70°). Fig. 11 illustrates the result for a simulated illumination from west. With the east, north combination more than 72% of the building roofs are undisturbed visible from at least one direction. Road coverage of 85% can be achieved by fusing four measurements. Concluding from the large viewing angle of the advantageous measurements layover seems to be the critical phenomenon for a task like building reconstruction.

In case of the roads the best result is achievable for an illumination from exactly north and west with a viewing angle of 45°. These directions coincide with the main road orientations. The third illumination direction is along the tilted long road from 210° anti-clockwise towards north (off nadir angle θ = 50°) and the fourth from east to west (θ = 60°). However, even in case of the fusion of four SAR images still more than a third of the road area can not be sensed.

C. *Detection of dominant line scatterers*

Besides layover and shadow dominant scattering is present in the data. These strong signal responses are in many cases caused from total reflection and double-bounce scattering. On the one hand these effects may be exploited as features for a building recognition, like the strong response at the dihedral corner between building and ground. On the other hand are objects in the neighborhood of such dominant scatterers often hardly visible. Fig. 12a shows a detail of the test data with strong signal at building locations. The locations of possible strong scattering (Fig. 12b) were detected by the analysis of 3D vector data derived from the LIDAR DEM. This time consuming analysis was carried out for one aspect.

IV. DISCUSSION AND OUTLOOK

The analysis of buildings and roads in urban areas is limited due to the SAR sensor principle. With a single SAR measurement useful data can be acquired usually for a minor part of the object areas only. It was shown that this limitation

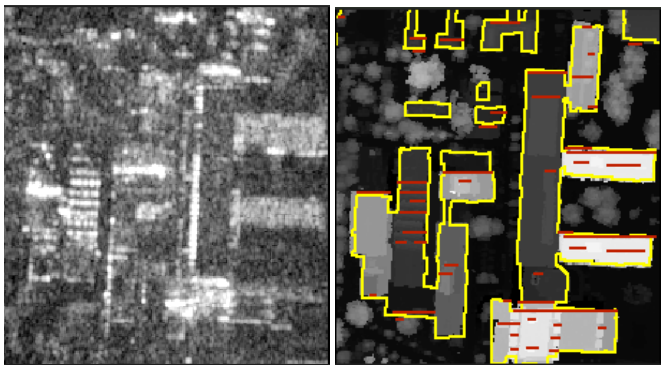

Fig. 12. a) SAR image, b) DEM with building footprints (yellow) and possible corner structures (red)

can be overcome by taking additional SAR data from different aspect and viewing angles into account. Particularly, in case of the buildings the improvement is significant: more than 80% of the roofs are visible combining data of three complementing illumination directions. This result encourages efforts to reconstruct buildings from SAR and InSAR data. On the other hand significant portions of the road area are not visible in spite of a fusion of several carefully chosen acquisition directions. In future work the detection of strong scatterers will be included in the framework to determine optimal SAR illumination aspects.

ACKNOWLEDGMENT

We thank Dr. Ender (FGAN-FHR) for providing the SAR data. The data were recorded by the AER II system of FGAN.

REFERENCES

[1] R. Bolter: Buildings from SAR: "Detection and Reconstruction of Buildings from Multiple View High Resolution Interferometric SAR Data", PhD. thesis, University Graz (Austria), 2001.

[2] M. Gelautz, H. Frick, J. Raggam, J. Burgstaller and F. Leberl: "SAR Image Simulation and Analysis of Alpine Terrain", ISPRS Journal of Photogrammetry and Remote Sensing, Vol. 53, 1998, pp. 17-38.

[3] E. Meier, U. Frei and D. Nüesch: "Precise Terrain Corrected Geocoded Images", In: Schreier G (ed.) SAR Geocoding: Data and Systems, Wichmann, Karlsruhe, 1993, pp. 173-185.

[4] G. Schreier: "Geometrical properties of SAR images", In: Schreier G (ed.) SAR Geocoding: Data and Systems, Wichmann, Karlsruhe, 1993, pp. 103-134.

[5] U. Soergel, U. Thoennessen, H. Gross and U. Stilla: "Segmentation of Interferometric SAR Data for Building Detection", IAPRS, Vol. 23, B 1, Amsterdam, 2000, pp. 328-335.

[6] U. Stilla and K. Jurkiewicz: "Reconstruction of Building Models from Maps and Laser Altimeter Data", In: P. Agouris and A. Stefanidis (eds.) Integrated Spatial databases: Digital Images and GIS, Berlin Springer, 1999, pp. 39-46.

[7] U. Stilla, U. Soergel, U. Thoennessen and E. Michaelsen: "Segmentation of LIDAR and INSAR Elevation Data for Building Reconstruction", In: E. P. Baltsavias, A. Gruen and L. Van Gol, (eds.) Automatic Extraction of Man-Made Objects from Aerial and Space Images (III), Balkema, Lisse, Netherlands, 2001, pp. 297-307.

[8] F. Tupin and M. Roux:" Markov Random Fields for Digital Terrain Model Extraction", Joint workshop on remote sensing and data fusion over urban areas, Urban 2001, 2001, pp. 95-99.